Progress In Electromagnetics Research C, Vol. 87, 227–240, 2018

Clutter Suppression for Cooperative Radar Based on Orthogonal Polarization Character

Maoqiang Jing, Zhuming Chen*, Qianli Wang, and Qi Jiang

Abstract—In indoor scenario, radar echoes are interfered by clutter from walls, ceilings, floors, and other indoor objects. Therefore, clutter suppressing is one of the key problems for indoor radar. This paper focuses on the problem of clutter suppressing for a secondary radar system which can be used in indoor localization. A clutter suppressing method based on orthogonal polarization character is presented. The orthogonal polarization character here is achieved by a designed transceiver, which can transpond electromagnetic waves in vertical polarization if and only if the received signal is in horizontal polarization. Thus the newly introduced polarization character can be used to discriminate target from clutter. Clutter is suppressed after calculating scattering similarity parameters via Pauli decomposition. Simulations and an experiment are conducted to demonstrate the proposed method. Compared with previous methods, the proposed method can distinguish stationary target with both static and varying clutters. Therefore, it is more practical for applications.

1. INTRODUCTION

The vast majority of radio-based indoor localization systems have the requirement that a tracked person carries an electronic device or tag [1–3]. These active localization techniques include WLAN (Wi-Fi), Ultra-WideBand (UWB), radio frequency identification (RFID) and radar [4–6]. Considering coverage, accuracy, and system cost, indoor radar has more advantages over other techniques [7, 8]. This paper focuses on clutter suppressing for a cooperative radar(secondary radar) system in indoor scenario.

The areas of utilization of indoor radar can be manifold, including target detection, localization, and tracking [9–11]. In an indoor scenario, radar echoes are interfered by clutter from walls, ceilings, floors, and other objects [12, 13]. Unlike sea clutter or ground clutter, clutter in indoor environment does not fluctuate and is not probabilistic, which leaves clutter suppressing methods in [14, 15] for conventional radar degraded. For this reason, clutter suppressing is one of the key problems for indoor radar.

In [9, 16, 17], several clutter suppressing methods are proposed for indoor radar. In [9], a clutter filtering method is presented, which uses a Kalman filter to estimate the indoor background clutter. Clutter is then suppressed after subtracting the estimated clutter map from received signals. In [16, 17], clutter suppressing method named empty room method is presented. This method estimates indoor background clutter under the assumption that the clutter is the average of a number of previous radar echoes.

The key concept of methods in [9, 16, 17] is to estimate background clutter $\overline{X_c}(t)$ from radar echo $X(t)$. Usually the estimated clutter $\overline{X_c}(t)$ is named as clutter map. Once the clutter map is calculated, background clutter is mitigated from received radar signal via $X(t) - \overline{X_c}(t)$. The main difference of methods in [9, 16, 17] is the various approaches to estimate $\overline{X_c}(t)$. Therefore, methods in [9, 16, 17] are the same kind of method. The drawbacks of this kind of method lie in:

Received 18 August 2018, Accepted 13 October 2018, Scheduled 25 October 2018
* Corresponding author: Zhuming Chen (zmchen@uestc.edu.cn).
The authors are with the University of Electronic Science and Technology of China, Chengdu, China.

(1) the performance of clutter suppressing is determined by the accuracy of clutter map estimating;
(2) clutter map requires being updated when indoor scenario varies, otherwise, the performance of clutter suppressing is degraded.

This paper aims at clutter suppressing for cooperative target in indoor scenario. A clutter suppressing method is proposed, which is based on the difference between cooperative target and clutter in scattering mechanisms. Clutter is suppressed directly according to the similarity parameter.

In order to provide a unique scattering mechanism for the cooperative target, the target in this paper is designed with orthogonal polarization character. This special character is achieved with the transceiver in the cooperative target, where receiving antenna is in horizontal polarization and transmitting antenna is in vertical polarization respectively. Therefore, with ideal cross-polarization isolation, the cooperative target can transpond electromagnetic waves in vertical polarization if and only if the received signal is in horizontal polarization.

Note: in this paper, cooperative target with this polarization character is noted as orthogonal polarization target.

Simulations and an experiment in a real scenario are conducted to demonstrate the proposed method. Compared with methods in [9, 16, 17], the proposed method does not require clutter map, and clutter is suppressed according to the differences in scattering mechanisms between target and clutter. Therefore, its performance stays robust with both static and varying clutter, which is more practical in applications.

The rest of this paper is organized as follows: Section 2 will sketch the scattering matrix theory and give definition for orthogonal polarization target; Section 3 will propose the clutter suppressing method; Section 4 will discuss the proposed method in indoor scenarios via simulation results; In Section 5, an experiment under a real indoor condition is conducted; results and discussions for both simulation and experiment are shown in Section 6 and finally, conclusions are drawn in Section 7.

2. SCATTERING MATRIX

The proposed method uses full-polarization information from radar echo. In polarimetric radar theory, radar transmitter is defined as a source of electromagnetic waves. Let vector $\vec{E}_t = [E_H^t, E_V^t]^T$ denote Jones vector for transmitted wave; $\vec{E}_r = [E_H^t, E_V^t]^T$ denote Jones vector for scattered wave; superscript ^{T} denote transposition; subscript H and V denote horizontal and vertical polarizations, respectively. Scattering matrix $[S]$ for radar target is defined as [19]:

$$\vec{E}_r = \frac{e^{-j\beta r}}{\vec{r}} [\ S\ ] \vec{E}_t \tag{1}$$

$$[\ S\ ] = \begin{bmatrix} s_{HH} & s_{HV} \\ s_{VH} & s_{VV} \end{bmatrix} \tag{2}$$

where r and $\vec{r}$ denote propagation path and propagation path vector, respectively, and β denotes wave propagation constant.

Scattering matrix $[S]$ of natural target follows the vector reciprocity principle of electromagnetic waves. When radar transmitter and receiver are at the same position, $s_{HV} = s_{VH}$ is satisfied in backscattering alignment (BSA) systems. A rigorous proof can be found in [19].

However, in this paper, the receiving antenna of the orthogonal polarization target is in horizontal polarization and transmitting antenna in vertical polarization, respectively. With ideal cross-polarization isolation, the scattering matrix of the orthogonal polarization target is:

$$[\ S\ ]_0 = \begin{bmatrix} s_{HH}^0 & s_{HV}^0 \\ s_{VH}^0 & s_{VV}^0 \end{bmatrix} = \begin{bmatrix} 0 & 0 \\ A \cdot e^{j\varphi} & 0 \end{bmatrix} \tag{3}$$

where A denotes the gain, and φ denotes the phase shift. Here, to make the analysis simplified, self-scattering or structural return of this target is neglected. In Section 5, a detailed and practical solution of this target will be presented.

As shown in Eq. (3), orthogonal polarization target violates reciprocity principle, because the orthogonal polarization target is cooperative and selectively receives electromagnetic waves in horizontal

polarization and transports electromagnetic waves in vertical polarization. Nevertheless, the scattering matrices of indoor clutter obey reciprocity principle, where $s_{HV} = s_{VH}$.

In indoor scenario, dihedral is ubiquitous, and clutter from rotated dihedral is composed with strong cross-polarization component. This cross-polarization character is similar to the orthogonal polarization target. Here, polarization signature in [19, 20] is used to address how scattering mechanism of orthogonal polarization target differs from dihedral. Let J_r and J_t denote Jones vectors for receiving and transmitting antenna polarization respectively, and σ_{rt}^0 denote backscattering coefficient for radar target, then the relationship between a given scattering matrix $[S]$ and its corresponding σ_{rt}^0 lies in [20]:

$$\sigma_{rt}^0(\psi_t, \chi_t, \psi_r, \chi_r) = \frac{4\pi}{a} \left| J_r^T [S] J_t \right|^2 \tag{4}$$

where $|\ |$ denotes the absolute value; a is a constant, which is relative to target size; (ψ_r, χ_r) and (ψ_t, χ_t) denote pairs of polarization ellipse angles for receiving and transmitting antennas, respectively; ψ_t and ψ_r denote ellipse orientation angle; χ_t and χ_r denote ellipticity angle.

Equation (4) is named as polarization signature, which is a function of transmitting and receiving antenna polarization $(\psi_t, \chi_t, \psi_r, \chi_r)$. This polarization signature is a graphical representation of received target intensity.

Figure 1 demonstrate polarization signatures for dihedral and orthogonal polarization targets, where the radar receiving antenna and transmitting antenna are co-popularized ($\psi = \psi_t = \psi_r,\ \chi = \chi_t = \chi_r$) and cross-polarized ($\psi = \psi_t = \psi_r + 90^\circ,\ \chi = \chi_t = -\chi_r$). According to Fig. 1(a) and Fig. 1(b), echoes from non-rotated dihedral do not contain cross-polarization component in linear polarization where $\chi = \chi_t = \chi_r = 0$. However, according to Fig. 1(d), echoes from 45° rotated dihedral are composed with strong cross-polarization component in linear polarization. As a result, cross-polarization component is caused by the rotation of dihedral. The rotated dihedral is ubiquitous in indoor scenarios.

As demonstrated in Fig. 1(d) and Fig. 1(f), echoes from orthogonal polarization target and 45° rotated dihedral can be received in VH polarization ($\psi_t = 0,\ \chi_t = 0,\ \psi_r = 90^\circ,\ \chi_r = 0$). However, polarization signatures of orthogonal polarization target and dihedral are different according to Fig. 1(e), Fig. 1(c), Fig. 1(f), and Fig. 1(d). Therefore, with full-polarization information (HH, HV, VH, VV), target can be discriminated from dihedral clutter.

3. CLUTTER SUPPRESSING METHOD

Radar one dimension range profiles are expressed as:

$$[\ S\ ]_n = \begin{bmatrix} s_{HH}^n & s_{HV}^n \\ s_{VH}^n & s_{VV}^n \end{bmatrix} \tag{5}$$

where $[S]_n$ denotes the scattering matrix for the n-th range bin, which is measured by the full polarized radar, and s_{HH}^n, s_{HV}^n, s_{VH}^n and s_{VV}^n are complex magnitudes for the n-th range bin in different polarizations (HH, HV, VH, VV). In indoor scenario, $[S]_n$ is composed of target and background clutter. The goal is to suppress clutter in $[S]_n$.

In order to discriminate target from clutter, Pauli decomposition is used here to calculate the similarity parameter [18]. The parameter is an indicator of polarization difference between target and clutter:

$$l\left([S]_n, [S]_0\right) = \frac{|k_n^H k_0|^2}{\|k_n\|_2^2 \|k_0\|_2^2} \tag{6}$$

where ^{H} denotes the complex conjugate, and $\|\ \|_2$ denotes the 2-norm of the vector. k_n and k_0 are the Pauli scattering vectors for radar range profiles:

$$k_i = \frac{1}{\sqrt{2}} \begin{bmatrix} s_{HH}^i + s_{VV}^i \\ s_{HH}^i - s_{VV}^i \\ s_{HV}^i + s_{VH}^i \\ j \cdot (s_{HV}^i - s_{VH}^i) \end{bmatrix} i = n, 0 \tag{7}$$

$l([S]_n, [S]_0)$ denotes the similarity parameter for the two scattering matrices $[S]_n$ and $[S]_0$. This similarity parameter does not vary with the orientation angles or with target sizes. The value of l is from 0 to 1, and $l = 1$ means that $[S]_n$ and $[S]_0$ are composed of the same scattering mechanisms [19].

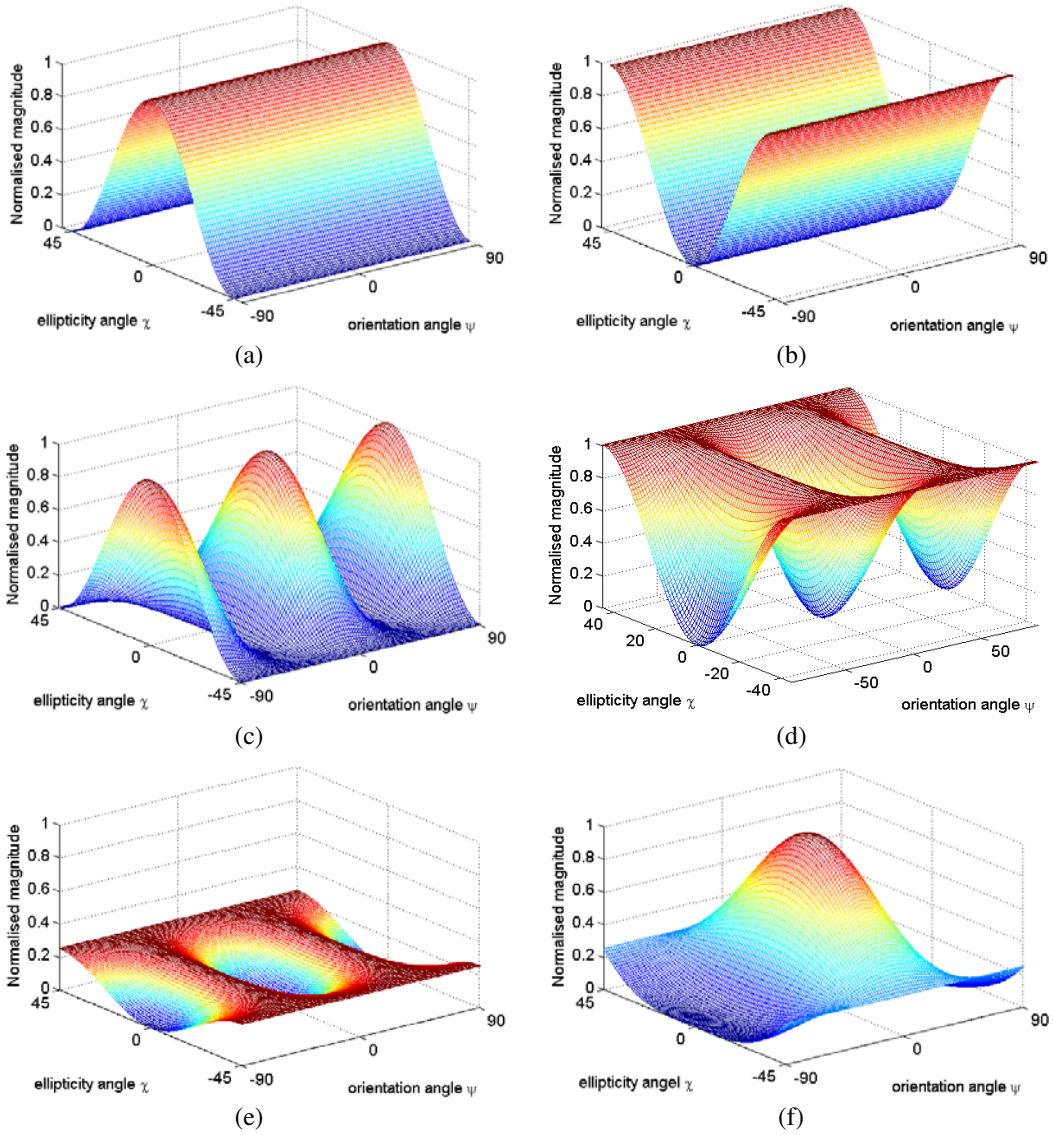

Figure 1. Polarization signatures of dihedral and orthogonal polarization targets (radar line-of-sight is parallel with the angle bisector of dihedral, and "normal" incidence is assumed): dihedral in (a) co-polarized, (b) cross-polarized; dihedral which is 45° rotated along radar line of sight in (c) co-polarized, (d) cross-polarized; orthogonal polarization target in (e) co-polarized, (f) cross-polarized.

We define a clutter suppression filter where radar range profiles are calculated:

$$\Psi(n) = \frac{1}{1 - l([S]_n, [S]_0)} \tag{8}$$

Ignoring some constant terms, we get:

$$\Psi_0(n) = \frac{|s_{VH}^n|^2}{|s_{HH}^n|^2 + |s_{HV}^n|^2 + |s_{VV}^n|^2} \tag{9}$$

According to Eq. (9), in noise-free condition, when the target is located at n-th range bin, $\Psi_0(n)$ is $+\infty$ due to $s_{HH}^0 = s_{HV}^0 = s_{VV}^0 = 0$ for $[S]_0$. Scattering mechanism of clutter can be decomposed as a combination of plane, dihedral, trihedral, etc., but none of these scattering mechanisms is similar to $[S]_0$ in Eq. (3), as shown in Table 1, because the reciprocal principle is always satisfied for indoor

clutter. If $[S]_n$ is only composed of clutter, $\Psi_0(r) \leq 1$. Therefore, $\Psi_0(n)$ can be regarded as an output of clutter suppression filter. A recommended threshold for target detection after clutter suppressing is $\Psi_0(r) > 1$, because reciprocity principle is violated only for orthogonal polarization target.

Note: The clutter suppressing process differs from conventional target detecting theory because polarization information in the proposed method is not probabilistic for both target and clutter. Therefore, clutter suppression in this paper is not a statistic or hypothesis testing problem.

Table 1. Different ideal scattering mechanisms and their magnitude after clutter suppressing, compared with orthogonal polarization target.

targets	s_{HH}	s_{HV}	s_{VH}	s_{VV}	magnitude
sphere	1	0	0	1	0
dihedral	1	0	0	-1	0
45° rotated dihedral	0	1	1	0	1
trihedral corner	1	0	0	1	0
left helix	-1	j	j	1	0.33
right helix	-1	$-j$	$-j$	1	0.33
orthogonal polarisation target(ideal)	0	0	$Ae^{j\phi}$	0	∞

It is worth mentioning that in conventional polarimetric radar theory [18, 19], $s_{HV} = s_{VH}$ is assumed. In Eq. (7), the cross-polarization component $j \cdot (s^i_{HV} - s^i_{VH})$ is ignored. However, in proposed method, the cross-polarization component must not be ignored due to $s_{HV} \neq s_{VH}$ in Eq. (3). Otherwise, the similarity parameter cannot discriminate orthogonal polarization target from cross-polarization clutter such as 45° rotated dihedral in Fig. 1(c) and Fig. 1(d).

4. SIMULATION

4.1. Simulation Model

In this section, simulations in different scenarios are conducted to compare the performances of the proposed method and methods in [9, 16, 17]. In each simulation, a linear frequency-modulated continuous-wave (LFMCW) radar and an orthogonal polarization target are put into a certain indoor scenario. In each simulation scenario, objects such as doors are changed, thus a varying scene is provided. Comparisons between the proposed method and methods in [9, 16, 17] under varying scenario conditions are presented.

Table 2 demonstrates the parameters of the LFMCW radar in each simulation. Compared with thermal noise, clutter in each scenario is the major problem. Therefore, thermal noise is ignored in the simulations.

Table 2. LFMCW radar parameters in this simulation.

radar parameters	value
center frequency	10 GHz
bandwidth	800 MHz
resolution	0.2 m
range bin	0.1 m
antenna horizontal beamwidth	15°
antenna vertical beamwidth	15°
polarization	HH, HV, VH, VV

Radar echoes are calculated via ray tracing method [21–23]. Ray tracing treats electromagnetic waves as ray tubes, then radar echoes at any location within indoor scenario are represented by a summation of rays reaching the location and reflecting back to radar [24, 25]. Both background clutter

and radar echo from the orthogonal polarization target can be calculated respectively through ray tracing method. Ray tracing method provides us with accurate information about indoor background clutter distribution and propagation path of radar signals.

Objects such as walls in each indoor scenario are relatively smooth, compared with radar wavelength, which is shown in Table 2. Therefore, the impact of wall roughness on ray propagation can be neglected [22]. In order to make the ray tracing process simplified, diffraction is ignored in this simulation. Walls are set to be perfect conductor so that background clutter rays in each scenario are reflected by walls. In this way, harsh indoor environments with severe background clutter interference are provided.

Ray tracing parameters in this section are shown in Table 3. In each simulation, electromagnetic rays are calculated through Wireless InSite software with the built in X3D ray tracing model, and most simulation parameters are set with default values in the software. After ray path calculating, radar 1-D range profiles are calculated with the following process:

Let $S(t)_{p,q}$ denote transmitted signal, and radar echo $R(t)_{p,q}$ is organized as:

$$R(t)_{p,q} = \sum_{m=1}^{M} \frac{e^{-j\beta r_m}}{r_m} S_{p,q}(t - r_m/c) \quad p = H, V; \quad q = H, V \tag{10}$$

where p and q denote the radar receive and transmit antenna polarizations, respectively; r_m is the m-th ray path; the overall ray number M for each scenario is 25; β is the wave propagation constant for $S(t)_{p,q}$. Then radar one dimension range profiles in full-polarization (s^n_{HH}, s^n_{HV}, s^n_{VH} and s^n_{VV}) can finally be calculated via matched filtering process respectively:

$$s_{p,q}(\tau) = \int R_{p,q}(t) S_{p,q}(t - \tau) dt \quad p = H, V; \quad q = H, V \tag{11}$$

where τ denotes the time delay and the measured range $r = \tau c/2$, and c denotes the light speed in free space.

Table 3. Ray tracing parameters in this section.

parameters	value
simulation software	Wireless InSite
propagation model	X3D ray
ray number	25
number of reflections	6
number of diffractions	1
ray spacing	0.25°

Methods in [9, 16, 17] are performed for comparison. Since methods in [9, 16, 17] are the same kind of methods which require clutter map estimation before clutter suppressing process, methods in [9, 16, 17] are treated as the same conventional method in this section. Clutter map can then be directly calculated after ray path calculation through Equation (10) in each simulation, because exact ray paths for radar signal propagation as well as indoor clutter distribution can be provided through ray tracing method.

Polarization information is not used in conventional method. Since the conventional method is based on energy distributions of clutter in range profiles, only VH polarization information is needed (other polarization information for orthogonal polarization target does not contain the direct wave). Although target in conventional method can be set in other polarization states, it can be easily demonstrated that if the target is co-polarized (i.e., receive antenna and transmit antenna are in the same polarization), the target and radar can be interfered by more severe co-polarized background clutter in indoor scenario. In order to make fair comparisons between the proposed method and conventional method, the target used in simulation process of conventional method is still the orthogonal polarization target.

4.2. Scenario A

Scenario A is a common scenario where indoor radar is widely used. In scenario A, the LFMCW radar and orthogonal polarization target are set in a $25\,\mathrm{m} \times 15\,\mathrm{m} \times 3\,\mathrm{m}$ room. Fig. 2 demonstrate a 3-dimension view of the room in door closed and door opened scenarios. Ceilings and floors are set to invisible so that the whole floor plan is visible. As shown in Fig. 2(a), radar and orthogonal polarization target are set at two corners in the room and are kept stationary respectively. Both target and radar are set 1.5 meters above the floor. The distance between radar and target is 27.5 meters. Moreover, the target is within radar line of sight to ensure that the direct wave is transmitted. By opening the doors in Fig. 2(a), the doors are replaced by free space in Fig. 2(b). As a result, the varying scenario is provided. In this way, flaws in conventional method can be demonstrated because for conventional method, clutter map requires being updated once the scenario changes.

Figure 3 demonstrates radar 1-D range profiles for background clutter in door opened and door closed scenarios respectively. In Fig. 3, radar antennas are set in VH polarization, and 1-D range profiles are calculated through Equations (10) and (11).

For conventional method, the clutter maps in each scenario are estimated before clutter suppression process. Because in this section, ray tracing method is used, clutter map can be calculated directly and precisely according to Fig. 3. Therefore, in this simulation, background clutter range profiles in Fig. 3 is used as clutter map for conventional method. Moreover, in order to demonstrate drawbacks of conventional method, background clutter in door closed scenario is treated as updated clutter map while clutter in door opened scenario is treated as original clutter map.

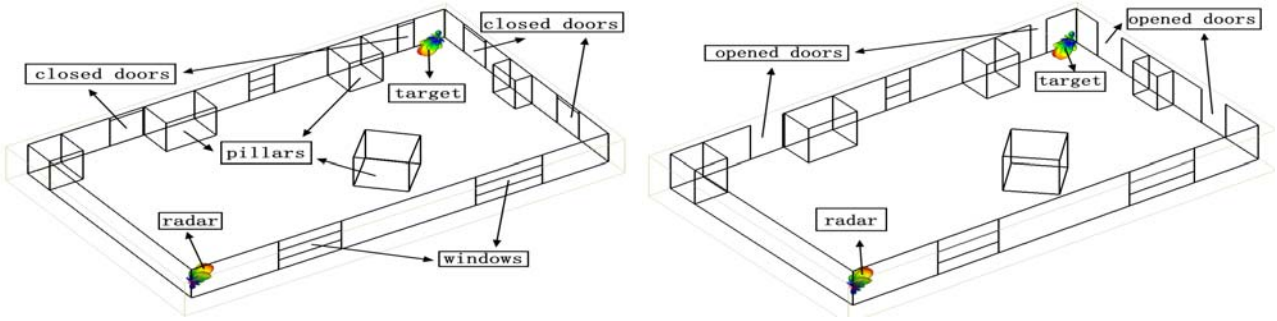

(a) (b)

Figure 2. 3-dimension view of the room in simulation scenario A. (a) Door closed scenario and (b) door opened scenario, radar and target are set at two corners in the room and 1.5 meters above the floor, the whole room is $25\,\mathrm{m} \times 15\,\mathrm{m} \times 3\,\mathrm{m}$, and the distance between radar and target is 27.5 meters.

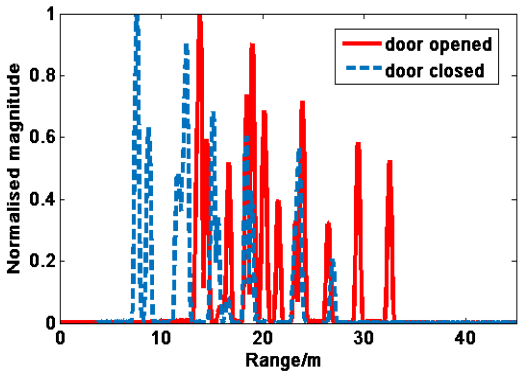

Figure 3. Background clutter for door opened and door closed scenarios in VH polarisation. Background clutter varies with scenario. For conventional method, clutter map must be updated from door opened scenario to door closed scenario.

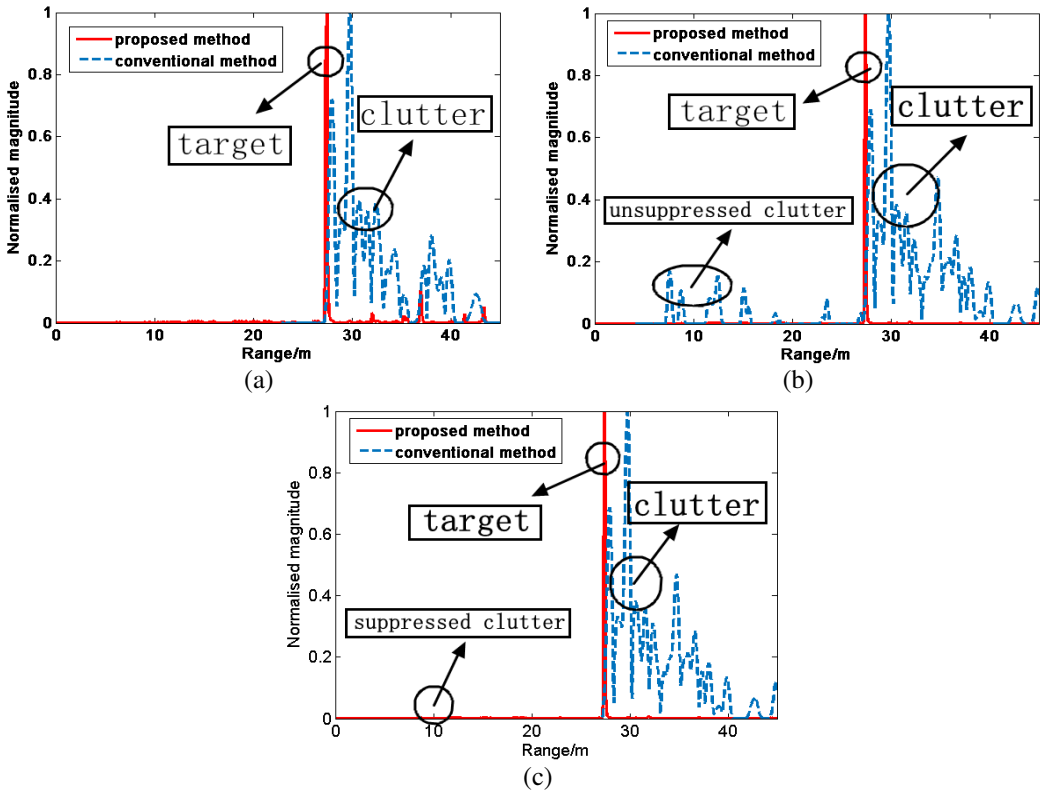

Figure 4. Clutter suppression results of proposed method and conventional method for (a) door opened scenario; (b) door closed scenario with original clutter map and (c) door closed scenario with updated clutter map.

Figures 4(a), 4(b) and 4(c) demonstrate clutter suppression results of the proposed method and conventional method in different scenarios. Conventional method is susceptible, according to Fig. 4(a) and Fig. 4(b). When scenario changes from doors opened to doors closed, unsuppressed clutter emerges because clutter map is not updated. After clutter map is updated, according to Fig. 4(c), part of the clutter is suppressed by conventional method.

One phenomenon worth mentioning is that, in this simulation, as demonstrated in Fig. 4, conventional method cannot mitigate clutters behind the target. Because the orthogonal polarization target is cooperative, electromagnetic rays in this scenario can be divided into two parts: background clutter rays and target rays. The unmitigated clutter comes from target rays which are emitted by radar and received by orthogonal polarization target and vise versa. Target rays here can be regarded as multipath. For conventional method, the estimated clutter map is from background rays, which are emitted by radar and reflected by walls, ceilings, floors or other indoor objects and finally received by the radar. Clutter map does not contain target rays, because it is estimated when target is removed from the scenario (or before target is added in the scenario). As a result, the performance of conventional method degrades.

4.3. Scenario B

Simulation in scenario B is conducted for further performance comparisons between the proposed method and conventional method. Scenario B is an indoor hallway, and the radar and orthogonal polarization target are put at either side of the indoor hallway, as shown in Fig. 5. The hall structure in this simulation scenario is similar to the scenario in the following experiment in a real hallway.

The whole scenario is in free space, which is the same as scenario A. The hallway is 3 meters high and 26 meters long. By opening the door from Fig. 5(a) to Fig. 5(b), a changing scenario is provided, where the door is replaced by free space (same as scenario A). The target and radar are both set 1.5 meters above the floor and kept stationary.

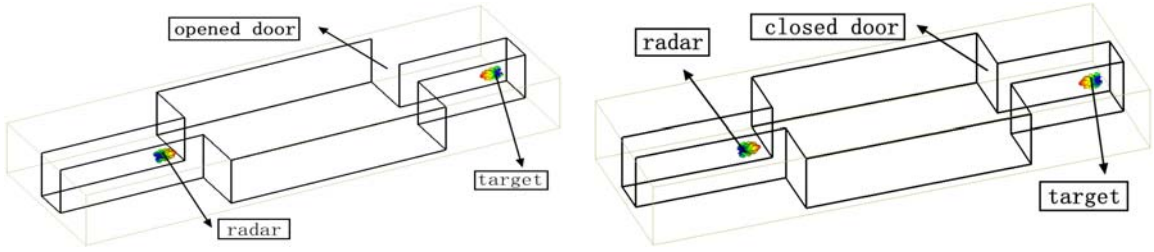

(a) (b)

Figure 5. 3-D view of the hallway of simulation scenario B in (a) door opened scenario, (b) door closed scenario. Radar and target are set at either side of the hallway and 1.5 meters above the floor. The whole hallway is 26 meters long and with a concrete wall at the end of the hallway, and the distance between radar and target is 19 meters.

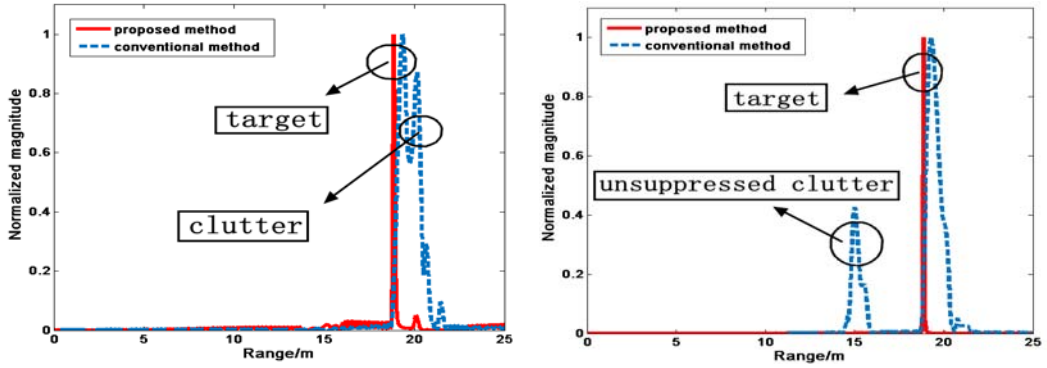

(a) (b)

Figure 6. Clutter suppression results of proposed method and conventional method for (a) door opened scenario; (b) door closed scenario with original clutter map. The proposed method stays robust while scenario varies.

Figure 6 shows clutter suppressing results of the conventional method and proposed method. Results in scenario B are in agreement with results of scenario A because clutter map is not updated when the door is closed. The performance of the conventional method becomes worse in Fig. 6(b), compared with door open scenario in Fig. 6(a). However, for the proposed method, the performance of clutter suppressing remains robust in this varying scenario.

5. EXPERIMENT

In this section, an experiment is conducted to further validate the proposed method. The experiment scenario is shown in Fig. 7. Both the radar and target were put into an indoor hallway and kept stationary. The floor plan of the hallway is shown in Fig. 8. The structure of hallway in this experiment is similar to the hallway in simulation scenario B while the hallway here is real, more complex and with more doors.

In this experiment, radar background clutter is caused by concrete walls and doors. Clutter distribution in this experiment can be changed by opening and closing the doors (same process as in scenario A and scenario B in the simulation section). Radar and target were both set 1 meter above the floor. The distance between radar and target was 32 meters. The dashed lines in Fig. 8 represent doors in the hallway, and doors can be set either opened or closed.

The experiment data for full-polarization 1-D range profiles were obtained by a simple LFMCW radar testing system. The test apparatus was composed of two parts: LFMCW radar and orthogonal polarization target. For radar, the two horn antennas in Fig. 7(a) can be switched into HH, HV, VH, VV modes and were used to obtain full-polarization information. The data in this experiment were

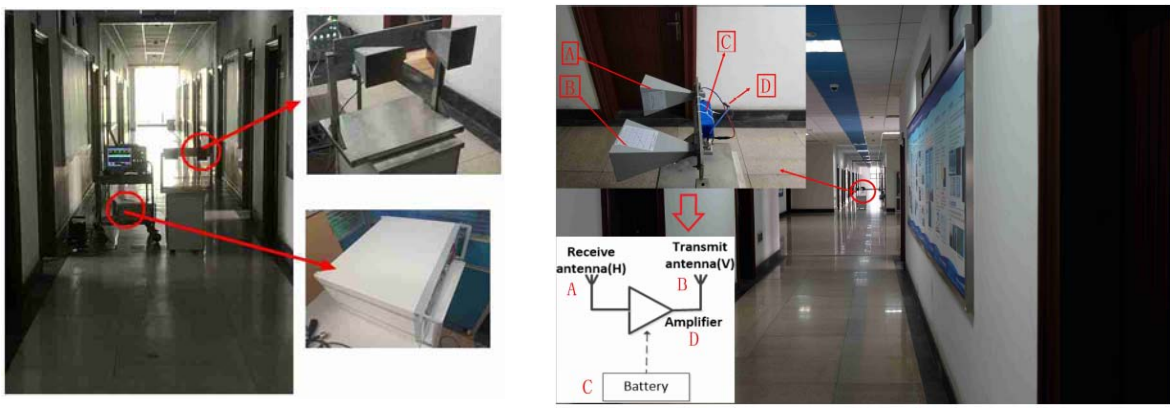

(a) (b)

Figure 7. Experiment scenes in a practical hallway. (a) LFMCW radar and radar antennas, (b) experiment scene and the scheme of the orthogonal polarization target. A: receiving antenna; B: transmit antenna; C: battery; D: amplifier.

Table 4. System parameters in this experiment.

system parameters	value
center frequency	10 GHz
bandwidth	400 MHz
range bin	0.2 m
antenna type	horn antenna
antenna horizontal beamwidth	15°
antenna vertical beamwidth	15°
radar polarization	HH, HV, VH, VV
target polarization	VH
target gain	10 dB

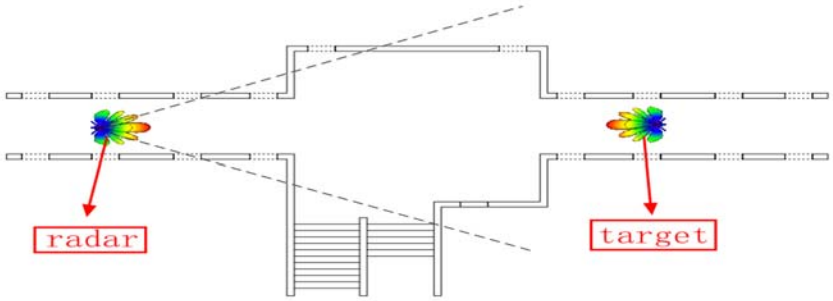

Figure 8. Floor plan of the experiment indoor hallway. Radar and target were both set 1 meter above the oor. The distance between radar and target is 32 meters. The dashed lines here represent doors in the hallway, doors can be set either opened or closed.

recorded via an oscilloscope. For the orthogonal polarization target, as shown in Fig. 7(b), two horn antennas were used and set in VH polarization (the receive antenna was in horizontal polarization and the transmit antenna in vertical polarization). In this experiment, antennas for radar and target were the same kind of horn antennas, as shown in Fig. 7. Therefore, a practical solution was achieved for the orthogonal polarization character. An amplifier with 10 dB gain was used in the target to further increase the signal to clutter ratio. Detailed system parameters are shown in Table 4.

In this experiment, methods in [9, 16, 17] were performed for comparison. Same as the simulation section, methods in [9, 16, 17] are treated as the same conventional method in this section. The clutter required for the conventional method was obtained by the following process: 1. shut down the battery power of the orthogonal polarization target; 2. record the background clutter; 3. estimate clutter map with processes in [9, 16, 17] according to radar 1-D range profiles. Fig. 9 shows the clutter maps in door opened and door closed scenarios. Fig. 10 shows the results after clutter suppressing process with the conventional method and proposed method. If the clutter map is not updated after the door is closed, unsuppressed clutter emerges in the conventional method in Fig. 10(b). However, for the proposed method, clutter suppressing performances remain the same in different scenes. The results are in agreement with simulation ones in scenario A and scenario B.

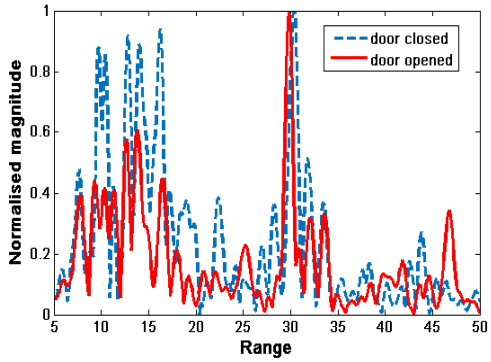

Figure 9. Background clutter for door opened and door closed scenarios in VH polarisation. Background clutter varies with scenario changing, thus for conventional method, clutter map must be updated from door opened scenario to door closed scenario.

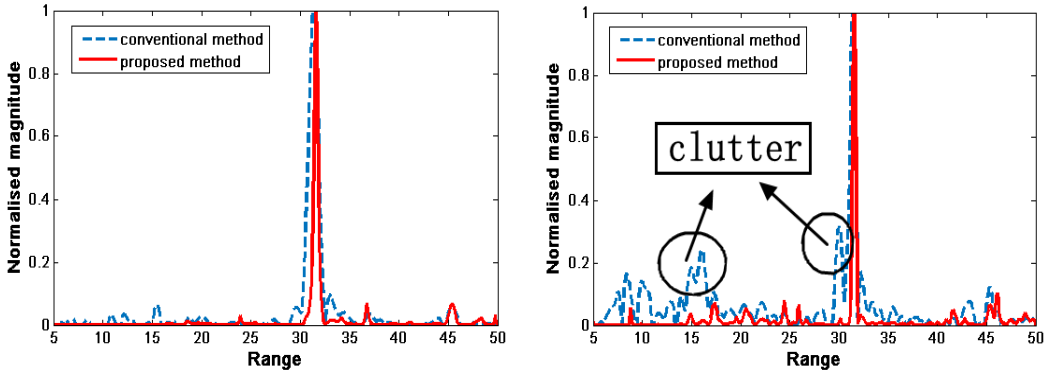

Figure 10. Clutter suppression results of proposed method and conventional method for (a) door opened scenario; (b) door closed scenario with original clutter map. Unsuppressed clutter emerges in (b) after conventional method while the proposed method stays robust while scenario varies.

6. RESULTS AND ANALYSES

As demonstrated in simulations and real experiment, the fault of methods in [9, 16, 17] is clear: the clutter map is required in advance, and the performance of clutter suppressing is vulnerable when scenario changes. However, in indoor condition, varying scenarios are inevitable due to the complexity of indoor environments. In the proposed method, clutter is suppressed according to different scattering mechanisms between clutter and target. This difference does not vary with scenarios.

Here we define the signal to clutter ratio improvement factor (ISCR) for further comparisons and describe clutter suppressing results quantitatively:

$$ISCR = \frac{SCR_{out}}{SCR_{in}} \tag{12}$$

where SCR_{in} denotes signal to clutter ratio before clutter suppression process, and SCR_{out} denotes signal to clutter ratio after clutter suppression process. For simulations in Section 4, both SCR_{in} and SCR_{out} can be directly calculated by summing the power of each ray, because each ray path and its power can be calculated precisely in ray tracing simulations. For the real experiment, both SCR_{in} and SCR_{out} are estimated in radar 1-D range profiles.

Table 5 demonstrates comparisons between the proposed method and conventional method (methods in [9, 16, 17]) in different scenarios (simulation scenarios A and B, real experiment scenario). ISCRs of the proposed method in simulation A and simulation B remain high, compared with conventional method. In different scenarios, ISCRs of the proposed method and conventional method vary because of different clutter distributions and clutter scattering mechanisms. Although both proposed method and conventional method show clutter suppressing improvement, ISCRs in real experiment are lower for both methods, because the real experiment is more complex than a simulation. This phenomenon may also be caused by the reliability of the experiment radar system.

ISCRs of the proposed method also depend on the scattering mechanisms of clutter. Therefore, in different clutter distribution conditions, ISCRs of the proposed method may vary. However, for the proposed method, it appears that the clutter suppressing results remain robust while background clutter varies. This advantage lies in polarization information and special scattering mechanism for orthogonal polarization target.

Table 5. Signal to clutter ratio improvement factors (ISCRs) in different scenarios for proposed method and conventional method.

scenarios	scene	methods	SCR_{in}/dB	SCR_{out}/dB	$ISCR$/dB
simulation scenario A	door opened	proposed method	−17.72	7.12	24.84
		conventional method	−17.72	−16.48	1.23
	door closed	proposed method	−18.73	16.80	35.53
		conventional method	−18.73	−17.43	1.29
simulation scenario B	door opened	proposed method	3.59	29.70	33.3
		conventional method	3.59	4.70	8.30
	door closed	proposed method	−0.46	37.93	38.40
		conventional method	−0.46	5.53	5.99
real experiment scenario	door opened	proposed method	−6.48	4.46	11.13
		conventional method	−6.48	−1.30	5.18
	door closed	proposed method	−14.43	−0.35	14.08
		conventional method	−14.43	−11.02	3.40

7. CONCLUSION

In this paper, a method for suppressing indoor clutter is proposed. By exploiting orthogonal polarization character, indoor clutter can be suppressed. The conducted simulations as well as real experiment results show that the proposed method shows better performance for varying indoor scenarios than previous indoor clutter suppressing methods [9, 16, 17]. The polarization information is used so that the proposed method does not require a prior knowledge of clutter. The proposed method is more practical for indoor applications. It is worth mentioning that the proposed method is not a stand-alone tool, but it is compatible. The modification of antennas can also be made for other radio-based indoor cooperative localization techniques. Therefore, the proposed clutter suppressing process is not limited for indoor radar. Although it increases the hardware complexity of localization system, the proposed solution shows more reliability in clutter suppressing process.

REFERENCES

1. Deak, G., K. Curran, and J. Condell, "A survey of active and passive indoor localisation systems," *Computer Communications*, Vol. 35, No. 16, 1939–1954, 2012.
2. Deak, G., K. Curran, and J. Condell, "History aware device-free passive (DfP) localisation," *Image Processing and Communications*, Vol. 16, No. 16, 21–30, 2011.
3. Farid, Z., R. Nordin, and M. Ismail, "Recent advances in wireless indoor localization techniques and system," *Journal of Computer Networks and Communicaitons*, Vol. 2013, Article ID 185138, 12 pages, 2013.
4. Rantakokko, J., J. Rydell, and P. Stromback, "Accurate and reliable soldier and first responder indoor positioning: Multisensor systems and cooperative localization," *IEEE Wireless Communications*, Vol. 18, No. 2, 10–18, 2011.
5. Mautz, R., "Indoor positioning technologies," *Habilitation Thesis*, ETH Zurich, Zurich, Switzerland, 2012.
6. Bahl, P. and V. N. Padmanabhan, "RADAR: An in-building RF-based user location and tracking system," *International Conference on Computer Communications*, Vol. 2, 775–784, Tel Aviv, Israel, 2000.
7. Chen, L., C. Wu, Y. Zhang, H. Wu, and C. Maple, "A survey of localization in wireless sensor network," *Int. J. Distrib. Sens. Netw.*, Vol. 8, No. 4, 385–391, 2012.
8. Parr, A., R. Miesen, and M. Vossiek, "Comparison of phase-based 3D near-field source localization techniques for UHF RFID," *Sensors*, Vol. 16, No. 7, 2016.
9. Nguyen, V. and V. Pyun, "Location detection and tracking of moving targets by a 2D IR-UWB radar system," *Sensors*, Vol. 15, No. 3, 6740–6762, 2015.
10. Peng, Z., J. Munozferreras, Y. Tang, R. Gomezgarcia, and C. Li, "Portable coherent frequency-modulated continuous-wave radar for indoor human tracking," *Proc. IEEE Topical Conf. Biomed. Wireless Technol., Netw., Sens. Syst. (BioWireleSS)*, 36–38, Austin, USA, Apr. 2016.
11. Mitilineos, S. A., D. M. Kyriazanos, O. E. Segou, J. N. Goufas, and S. C. A. Thomopoulos, "Indoor localization with wireless sensor networks," *Progress In Electromagnetics Research*, Vol. 109, 441–474, 2010.
12. Munozferreras, J., Z. Peng, R. Gomezgarcia, et al., "Isolate the clutter: pure and hybrid Linear-Frequency-Modulated Continuous-Wave (LFMCW) radars for indoor applications," *IEEE Microwave Magazine*, Vol. 16, No. 4, 40–54, 2015.
13. Tivive, F. H., A. Bouzerdoum, and M. Amin, "A subspace projection approach for wall clutter mitigation in Through-the-Wall radar imaging," *IEEE Trans. Geosci. Remote Sens.*, Vol. 53, No. 4, 2108–2122, 2015.
14. Ash, M., M. Ritchie, and K. Chetty, "On the application of digital moving target indication techniques to Short-Range FMCW radar data," *IEEE Sensors Journal*, Vol. 18, No. 10, 4167–4175, 2018.
15. Pourmottaghi, A., M. R. Taban, and S. Gazor, "A CFAR detector in a nonhomogenous weibull clutter," *Trans. Aerosp. Electron. Syst.*, Vol. 48, No. 2, 1747–1758, 2012.
16. Lee, B. H., S. Lee, and Y. J. Yoon, "Adaptive clutter suppression algorithm for human detection using IR-UWB radar," *IEEE SENSORS*, 1–3, Glasgow, UK, Oct. 2017.
17. Valmori, F., A. Giorgetti, and M. Mazzotti, "Indoor detection and tracking of human targets with UWB radar sensor networks," *IEEE Int. Conf. Ubiquitous Wireless Broadband (ICUWB)*, 1–4, Nanjing, China, Dec. 2016.
18. Yang, J., Y. N. Peng, and S. M. Lin, "Similarity between two scattering matrices," *Electron. Lett.*, Vol. 37, No. 3, 193–194, 2001.
19. Cloude, S. R., *Polarisation: Applications in Remote Sensing*, Oxford Univ. Press, London, U.K., 2009.
20. Van Zyl, J. J., H. A. Zebker, and C. Elachi, "Imaging radar polarisation signatures: Theory and observations," *Radio Science*, Vol. 22, 529–543, 1987.

21. Yun, Z. and M. F. Iskander, "Ray tracing for radio propagation modeling principles and applications," *IEEE Access*, Vol. 3, 1089–1100, 2015.
22. Zhou, C., "Ray tracing and modal methods for modeling radio propagation in tunnels with rough walls," *IEEE Transactions on Antennas and Propagation*, Vol. 65, No. 5, 2624–2634, 2017.
23. Tayebi, A., J. Gomez, F. M. S. D. Adana, and O. Gutierrez Blanco, "The application of ray-tracing to mobile localization using the direction of arrival and received signal strength in multipath indoor environments," *Progress In Electromagnetics Research*, Vol. 91, 1–15, 2009.
24. Blas Prieto, J., P. Fernandez Reguero, R. M. Lorenzo, E. J. Abril, and S. Mazuelas Franco, A. Bahillo Martinez, and D. Bullid, "A model for transition between outdoor and indoor propagation," *Progress In Electromagnetics Research*, Vol. 85, 147–167, 2008.
25. Martinez, D., F. Las-Heras Andres, and R. G. Ayestaran, "Fast methods for evaluating the electric field level in 2D-indoor environments," *Progress In Electromagnetics Research*, Vol. 69, 247–255, 2007.